

# SETI Investigations at Jodrell Bank, England: September Through November 1983

G. S. Downs

Communications Systems Research Section

S. Gulkis

Atmospheric Sciences Section

*The RFI environment at the Nuffield Radio Astronomy Laboratories was examined extensively in the frequency band 1404 to 1444 MHz using the DSN Advanced Systems' Radio Frequency Interference Surveillance System. An uncooled FET amplifier (62 K system temperature) was placed on the newly acquired 12.8-m antenna, and unlimited observing time was made available to the SETI project. One night of observing at 1667 MHz was made available on the 76-m antenna. Preliminary results of four investigations are reported here: (1) full scans of the horizon, cataloging RFI events between 1404 and 1444 MHz; (2) lunar reflections of terrestrial RFI signals between 1424 and 1444 MHz; (3) noise background (spectral baseline) distortions caused by galactic neutral hydrogen emission at 1420.4 MHz; (4) low sensitivity search for spectral features of F, G, and K stars.*

## I. Introduction

Several groups of scientists and engineers in the United States are cooperatively devising plans to carry out a major, systematic search for radio signals of extraterrestrial origin. This search for extraterrestrial intelligence (SETI) is sponsored by the Office of Life Science within the NASA, with most of the effort concentrated at the Ames Research Center (ARC) of NASA and at JPL. The intent is to search the 1- to 10-GHz microwave band using a special purpose digital spectrum analyzer at existing radio telescopes. This analyzer will provide more than  $10^6$  channels with a spectral resolution up to 1 Hz. A prototype spectrum analyzer is being constructed at Stan-

ford University that will provide 65,000 ( $2^{16}$ ) channels with simultaneous resolutions of 1, 32, and 1000 Hz, and total power.

Field tests have begun using an existing  $2^{16}$ -channel spectrum analyzer (Ref. 1 and Morris and Wilck, private communication), built at JPL originally as a radio frequency interference (RFI) surveillance system (RFISS). This device is limited to one spectral resolution, though it is now variable between 1 and 300 Hz. Both the JPL and Stanford spectrum analyzers will be used over the next five years to test hardware concepts, detection algorithms, and search strategies.

Of particular interest are the presence and character of RFI at potential observing sites. These interfering signals, not catalogued in advance, will cause long hours of delay while observers study a particular signal to determine whether it is of terrestrial origin, from a regularly passing satellite, or indeed from beyond the solar system. A frequency band of particular interest to SETI observers is that between emission lines at 1420 (HI, or neutral hydrogen) and 1667 MHz (OH radical). During September through November 1983, the Nuffield Radio Astronomy Laboratories at Jodrell Bank, England, made available to the SETI project a large amount of observing time on a new, moderately sensitive radio telescope at frequencies near 1420 MHz. This opportunity came at a time when field tests were just beginning, and the required time was not available at other observatories. Furthermore, the NASA Goldstone facility, where much field testing will be performed, does not yet have a receiving capability below 2250 MHz, and will not have this for at least one more year.

Therefore, the JPL mobile spectrum analyzer was shipped to Jodrell Bank for several weeks (1) to collect data on the RFI environment at a major observatory in a frequency band of critical importance, and (2) to determine how to improve the methods and associated software used to collect RFI data. To this end, the observing plan included the following activities:

- (1) Using the 12.8-m telescope, scan the entire horizon at frequencies between 1420 and 1667 MHz as allowed by the current receiver.
- (2) Explore, using the 12.8-m telescope, the RFI environment reflected by the Moon, and compare this with the known local environment.

Furthermore, several activities were planned that impact SETI search strategies:

- (3) Obtain HI spectra at high spectral resolution (30 to 60 Hz) in selected regions of the Galaxy. (The question of baseline problems related to the presence of HI over a wide frequency band will be explored with this data).
- (4) Obtain spectra at high resolution of F, G, and K stars located within 25 parsecs of the Sun. (A preliminary "eavesdropping" activity at a relatively low sensitivity.)

## II. The Measurement System

The receiving system consisted of an uncooled FET amplifier mounted on the newly arrived 12.8-m antenna, providing a system temperature  $T_s$  of approximately 62 K in left-circular polarization at 1420 MHz. This value was obtained by observing the HI source S7 (peak brightness temperature of 80 K; R. D. Davies, private communication). Assuming the source is

unresolved by the  $1.4^\circ$  beam (R. Pritchard, private communication),  $T_s \sim 125$  K was obtained. Assuming an aperture efficiency of 0.5,  $T_s \sim 62$  K. These assumptions require verification. The effective operating bandwidth was 1370 to 1440 MHz, the lower frequency determined by the receiver pass-band, and the upper frequency by the presence of a strong microwave link signal at 1457.625 MHz (the Mow Cop to Risley link).

The intermediate frequency (IF) signal from the Jodrell Bank system was passed on to an IF system in the NASA van (Fig. 1). It is the unique function of the JPL IF system to provide two signal channels of 10-MHz bandwidth, each with an in-phase (or real) and a quadrature (or imaginary) component. The system is usually used such that each channel samples a full 10 MHz of the IF passband. The two channels may be overlapping in frequency but represent two different polarizations (as in some of the OH observations reported below), or they may represent two contiguous portions of the same IF band (as in the RFI studies reported below).

Digitization for subsequent Fourier transformation was performed by four A/D converters. The hardware computation of the Fourier transform was done using the fast Fourier transform (FFT) algorithm. In fact, two independent  $2^{15}$ -sample transforms were computed simultaneously, yielding a total of  $2^{16}$  spectral points. The computations were pipelined, so that the usual two-dimensional butterfly diagram for the FFT algorithm must here be viewed as a three-dimensional diagram, with time the third dimension.

Running at the maximum rate (10-MHz bandwidth in each channel), a complete set of spectral points was computed every 3.2 ms. Subsequently, the real ( $V_r$ ) and imaginary ( $V_i$ ) components of the spectrum were combined to form the power spectrum ( $V_r^2 + V_i^2$ ). These spectra were accumulated in a separate memory, to be read later by the controlling computer (Modcomp II) for storage on magnetic disk and tapes.

## III. Low-Elevation Azimuth Scans

The 12.8-m radio telescope was used to scan  $360^\circ$  of horizon (elevation  $10.0^\circ$ ) in several 10-MHz frequency bands. The volume of data and lack of automation precluded analyzing all the data during the visit to Jodrell Bank; however, partial results for the 1404- to 1414-MHz and the 1414- to 1424-MHz bands were obtained and are summarized in Table 1 and Fig. 2. The analysis summarized here resulted from a visual inspection of 664 spectral plots, each with a resolution of 16 kHz. (A compression of 53 is used in displaying most of the spectra, wherein the *maximum* value in each 16-kHz bin is displayed). The frequencies listed in Table 1 should therefore be considered reliable to within 50 kHz.

The number of RFI events encountered at each azimuth in the frequency bands of 1404 to 1414 and 1414 to 1424 MHz are presented in Fig. 2. (A complete data set has been collected for the bands 1424 to 1434 and 1434 to 1444 MHz, but the analysis has been deferred until the appropriate software exists). A major difficulty in characterizing RFI is readily apparent: *time variability*. It is unlikely near 1420 MHz that this variability is due to the source being an artificial satellite, but this possibility should always be kept in mind. The spatial correlation noted in Table 1 and suggested in Fig. 2 is undoubtedly due to the colocation of several transmitters (e.g., a microwave tower). In addition, several weaker signals in a particular direction may be merely modulation sidebands of the major signal in that direction.

Most signals appeared over a range of azimuth much larger than the primary antenna beam (approximately  $1.4^\circ$ ). Several frequencies noted in Table 1 were seen over  $180^\circ$  of azimuth or more. We can only conclude that strong signals, surrounding hills, and local structures conspire to make some RFI inescapable. The one signal noted in Table 1 seen at all azimuths may be a signal generated within the receiver, though we observed a varying signal level in this case.

The conclusions to date are:

- (1) Several *days* of observing are required upon arrival at a new observatory to build up a catalog to RFI events.
- (2) The analysis of the RFI data must be automated, with particular attention to baseline removal in the presence of RFI, and to the appropriate threshold for cataloging an event such that true extraterrestrial signals are *not* included in the catalog.
- (3) The catalog will necessarily grow as the survey proceeds and the sensitivity to weak signals increases.

Examples of spectra contaminated by RFI appear in Figs. 3 through 6. A modest, typical level of RFI is apparent in Fig. 3. Note, however, the presence of a signal within 300 kHz of the broad H1 feature, well within the protected radio astronomy band. A more severe but not unusual level of RFI appears in Fig. 4. (The central peaks in all of these spectra are the result of a nonzero DC component in the signals presented to the A/D converters and should be ignored.) An unusually severe case is presented in Fig. 5, where several of the signals are clearly related to the strong interference near 1408.6 MHz. That same signal is presented in Fig. 6 at 16-kHz and 300-Hz resolution. These data were collected on two distinct days, partially illustrating time variations in the signal structure. Furthermore, the complexity and breadth of the signal are clearly brought out. Throughout the preliminary examination of these spectra, many exciting and unique examples of telem-

etry signals were found. A larger gallery of these snowflakes of the electromagnetic spectrum is clearly feasible, but such an endeavor is left to the final report.

To complete these observations, the frequency band 1404 to 1444 MHz was repeatedly monitored in 20 MHz blocks in long azimuth scans, each at an elevation of  $10.0^\circ$ , so that each azimuth was examined *several* times at each frequency. The scans proceeded slowly ( $0.2^\circ/\text{min}$ ), requiring 7 min to scan one beamwidth ( $1.4^\circ$ ). Thus 21 hours were required to fill the disk storage with 180 spectra while covering  $250^\circ$  in azimuth. (In fact, the scans proceeded at a much slower rate because of hardware difficulties and the considerable software development required to handle the data tapes properly.)

#### IV. Lunar Reflections of RFI

It may be possible to use the Moon to observe RFI generated around the globe. This technique is subject, however, to very severe restrictions. Let us compare a signal observed locally with a similar signal reflected from the Moon. The locally or directly observed signal will yield a receiver power  $P_d$  of

$$P_d = \frac{P_T G_T(\theta_d) A}{4 \pi D^2}$$

where

$P_T$  = transmitter power

$G_T(\theta_d)$  = transmitter antenna gain at angle  $\theta_d$  relative to the beam axis

$A$  = effective antenna aperture

and

$D$  = distance to the transmitter

However, the power  $P_r$  received via lunar reflections becomes

$$P_r = \frac{P_T G_T(\theta_r) \sigma A}{(4\pi)^2 R^4}$$

where

$\sigma$  =  $\sigma$  (reflecting area, roughness, dielectric constant)

= radar cross section

and

$R$  = the Earth-Moon distance

(We assume here that since angles of incidence and reflection are  $\sim 1^\circ$ , the quasi-specular component of backscatter is in fact observed.) The ratio of these two received powers becomes

$$\frac{P_r}{P_d} = \frac{G_T(\theta_r)}{G_T(\theta_d)} \frac{\sigma D^2}{4\pi R^4}$$

Taking  $\sigma \sim 0.07 \times (\text{projected lunar area}) \sim 6.7 \times 10^5 \text{ km}^2$ ,  $D \sim 50 \text{ km}$ , and  $R^4 \sim 2.1 \times 10^{22} \text{ km}^4$ , we obtain

$$\frac{P_r}{P_d} \sim 6.4 \times 10^{-15} \frac{G_T(\theta_r)}{G_T(\theta_d)}$$

representing a nominal loss of  $-142 \text{ dB}$ . If we observe  $P_d$  in a sidelobe where  $G_T(\theta_d) \sim 10^{-4} G_T(0)$ , and if  $\theta_r \sim 0$  (direct transmission to the Moon), then  $P_r$  is only about 100 dB down from the signal observed locally. By various combinations of  $\theta_r$  and  $\theta_d$  we can see that lunar reflections will be 100 to 180 dB lower than those observed locally.

Nevertheless, estimates of the expected signal-to-noise (S/N) ratio expected for large communications antennas are at first surprisingly encouraging. We expect

$$S/N = \frac{P_r}{kT_s \sqrt{\tau \Delta f}}$$

where  $T_s$  = the system temperature,  $\Delta f$  = the channel bandwidth, and  $\tau$  = the integration time. Taking  $G_T(0) \sim 55 \text{ dB}$  (a 26-m antenna at 21-cm wavelength),  $P_T \sim 1 \text{ kW}$ ,  $A \sim 3.2 \times 10^{-6} \text{ km}^2$  (assuming an aperture efficiency of 0.5), and letting  $g_T(\phi) = G_T(\phi)/G_T(0)$ , then

$$S/N = 3 \times 10^7 g_T(\phi) \tau^{1/2}$$

Naturally, the probability of a signal being directed at maximum gain towards the Moon is extremely low. Viewing leakage through sidelobes is considerably more probable. The expected S/N ratio for a range of sidelobe responses for both  $P_T = 1 \text{ kW}$  and  $100 \text{ W}$  are summarized in Table 2. We have considered the transmitter power to be concentrated in one narrow channel in constructing this table. Clearly, the power would be divided among several channels, decreasing the probability of detection correspondingly.

Because of lunar libration, the reflected signals can be Doppler broadened as much as 20 Hz at 1420 MHz. Thus, a finer resolution ( $\sim 30 \text{ Hz}$ ) is appropriate. However, these early

observations were performed at the coarsest (300-Hz) resolution since our lack of experience in this technique does not justify confining the bandwidth to obtain only a modest improvement in sensitivity. All of the spectra examined in this preliminary study are confined to the 1424- to 1444-MHz frequency band. Few contained signals. Nevertheless, some signals were observed at high elevations ( $\sim 50^\circ$ ), and an example is shown in Fig. 7. Two possible reflections are expanded to 300-Hz resolution in Fig. 8. A stronger statement on the source of these signals must await the analysis of the azimuth scans in this (1424- to 1444-MHz) frequency band. (While a preliminary analysis is available of the 1404- to 1424-MHz band, time permitted only cursory checks of the data quality in the higher frequency band.)

## V. Galactic Spectra

Narrow HI features (width  $\sim 1 \text{ kHz}$ ) are not known to exist. The sharpness of these features relative to the spectral undulations imposed by receiver filters can be bothersome, however, if not anticipated in baseline-removal schemes. Therefore, some higher resolution (64-Hz) data in the 2-MHz band surrounding the HI line (1420.4 MHz) was collected at several galactic longitudes. An example is shown in Fig. 9(a), where 5 minutes of integration at  $(\ell, b) = (0.0^\circ, 0.0^\circ)$  yielded a relatively complicated structure. A higher resolution view in Fig. 9(b) of the central region of one HI clump reveals no sharp surprises.

## VI. F, G, and K Stars

The F, G, and K class stars bracket the Sun in size and temperature, and are therefore prime candidates for life-containing planets. Certain K stars are flare stars, creating harsh circumstellar conditions, and should not be included in the list (B. Lovell, private communication). The investigations at Jodrell Bank were limited to those previously examined at OH frequencies at Arecibo and whose spectra suggested sharp features may be present (J. Tarter, private communication). A night of Mark IV (76-m diameter) telescope observing was provided by R. J. Cohen to study four objects (star list #9100 and #9220B, Orion and Venus) in both left- and right-circular polarizations with a spectral resolution of 300 Hz. No sharp features were observed.

(The spectral studies by R. J. Cohen of OH emission in certain regions were supplemented using the RFISS with 20-MHz spectra at 300-Hz resolution and with dual-polarization 2-MHz spectra at 60-Hz resolution.)

Hydrogen emission was observed with the 12.8-m telescope in two objects, RGO 672 and Vega, with a resolution of 64 Hz. The velocity of the emission in RGO 672 was similar to that previously published, and no sharp feature was seen at the

frequency suggested by the Arecibo observations. Two clumps of HI emission were observed in Vega at  $\sim 15$  and  $\sim 25$  km/s (relative to the local standard of rest), and no sharp features were observed.

## Acknowledgments

Many members of the staff at Jodrell Bank contributed to this series of measurements, and to them the SETI project is deeply indebted. Participants at Jodrell Bank from elsewhere were G. Downs, R. Emerson, M. Grimm, S. Gulkis, and G. Stevens of JPL, and J. Tarter of ARC and UC Berkeley.

## References

1. Morris, G. A., Jr., and Wilck, H. C., "JPL 2<sup>20</sup> Channel 300 MHz Bandwidth Digital Spectrum Analyzer," in *Deep Space Network Progress Report 42-46*, Jet Propulsion Laboratory, Pasadena, California, 1978, pp. 57-61.

**Table 1. Discrete RFI frequencies obtained in the 1404–1424 MHz band**

| Frequency<br>(1404-1414),<br>MHz | Frequency<br>(1414-1424),<br>MHz |
|----------------------------------|----------------------------------|
| 1404.108                         | 1414.068                         |
| 1404.863                         | 1414.772                         |
| 1404.909                         | 1414.818                         |
| 1405.454                         | 1414.909                         |
| 1406.107                         | 1415.045                         |
| 1406.363                         | 1415.127 <sup>c</sup>            |
| 1406.803                         | 1416.272                         |
| 1407.045 <sup>a</sup>            | 1416.500                         |
| 1407.954                         | 1417.678                         |
| 1408.090                         | 1417.714                         |
| 1408.590 <sup>a</sup>            | 1418.489                         |
| 1409.402 <sup>b</sup>            | 1418.768                         |
| 1409.500                         | 1419.863                         |
| 1409.590                         | 1420.000                         |
| 1409.909                         | 1420.090                         |
| 1409.955                         | 1420.199                         |
| 1410.000 <sup>c</sup>            | 1422.090                         |
| 1410.202 <sup>b</sup>            | 1422.498 <sup>c</sup>            |
| 1410.590                         | 1422.909                         |
| 1410.727                         | 1423.068                         |
| 1410.879                         | 1423.227                         |
| 1411.068                         |                                  |
| 1411.591                         |                                  |
| 1411.800                         |                                  |
| 1411.954                         |                                  |
| 1412.136                         |                                  |
| 1412.973                         |                                  |

<sup>a</sup>Peaks near azimuth 130° to 132°, and contains considerable sideband structure.

<sup>b</sup>These frequencies appear with the 1408.590 signal and may be more than spatially correlated with it.

<sup>c</sup>Occurs over an azimuth range greater than 180°.

**Table 2. Required integration time ( $\tau$ ) S/N ratio = 20**

| Sidelobe<br>response<br>$g_T(\phi)$ , dB | Integration Times |               |
|--|-------------------|---------------|
|  | $P_T = 1$ kW      | $P_T = 100$ W |
| -80                                      | 70 min            | 4.6 d         |
| -70                                      | 40 s              | 1.1 h         |
| -60                                      | 0.4 s             | 40 s          |
| -50                                      | 4 ms              | 0.4 s         |
| -40                                      | 40 $\mu$ s        | 4 ms          |
| -30                                      | 0.4 $\mu$ s       | 40 $\mu$ s    |

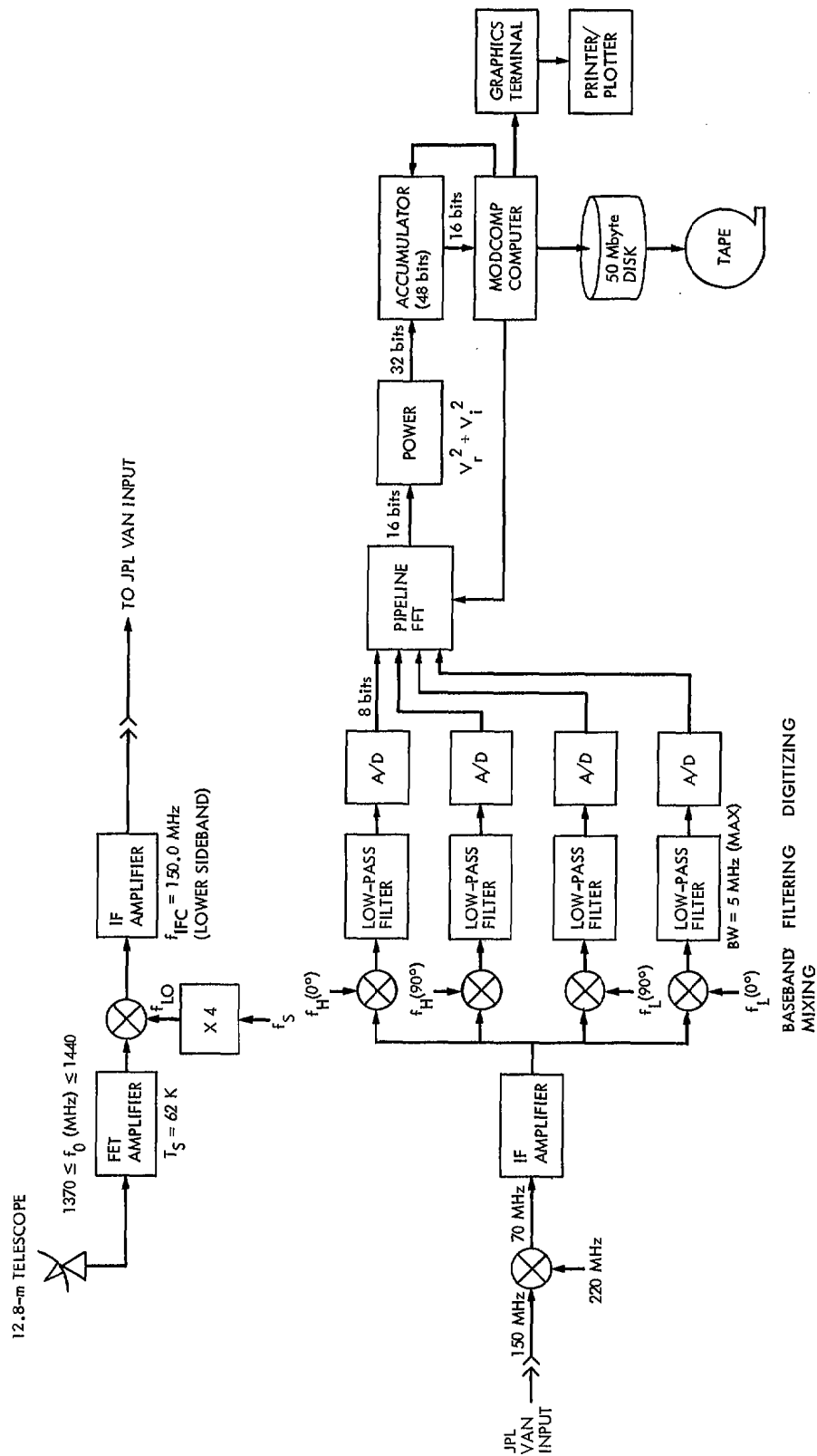


Fig. 1. The spectrometer system at Jodrell Bank

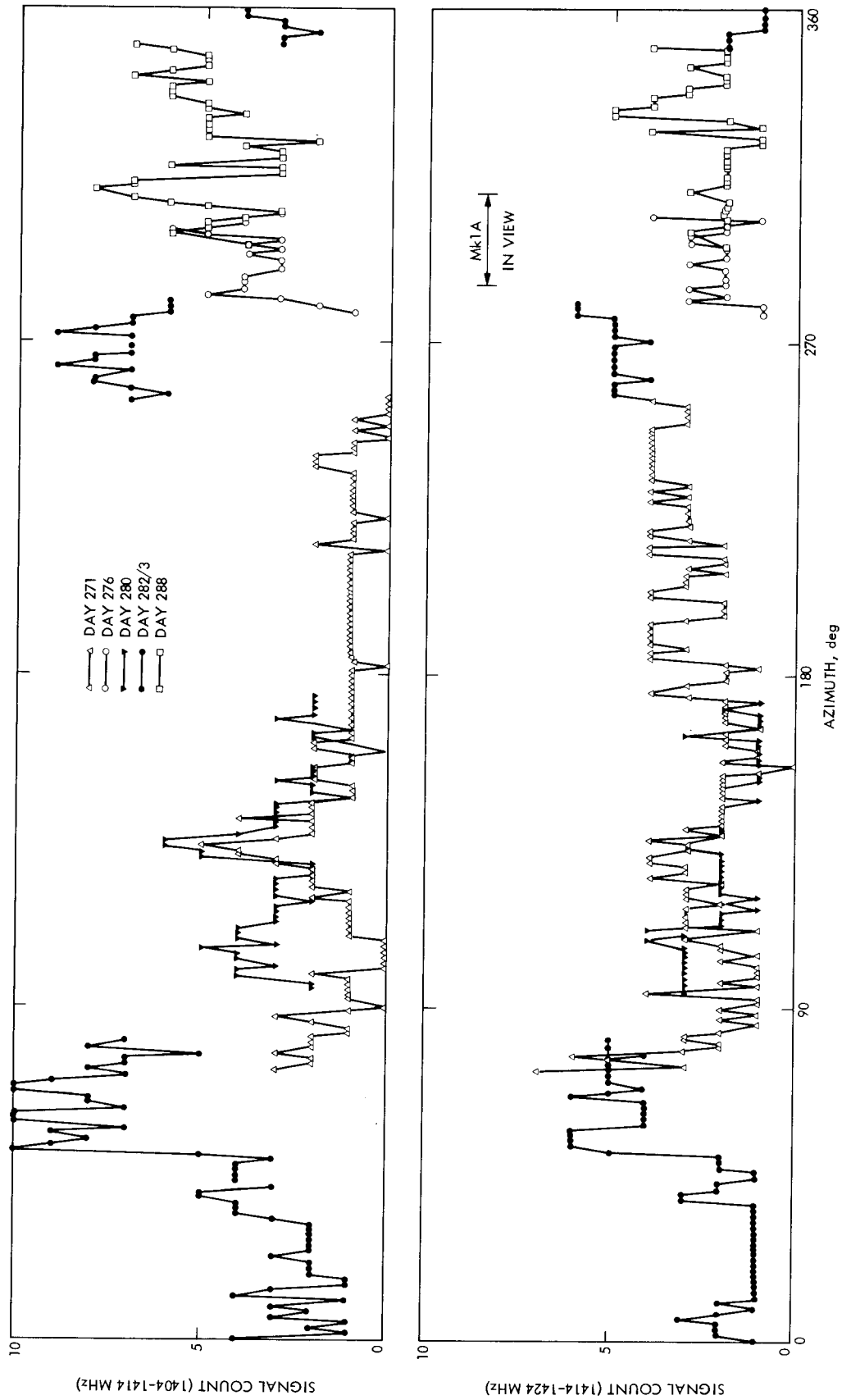
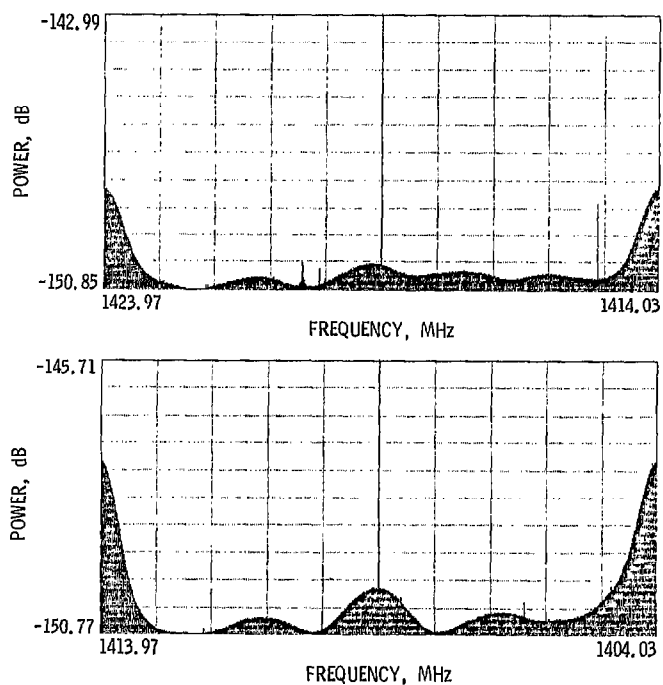
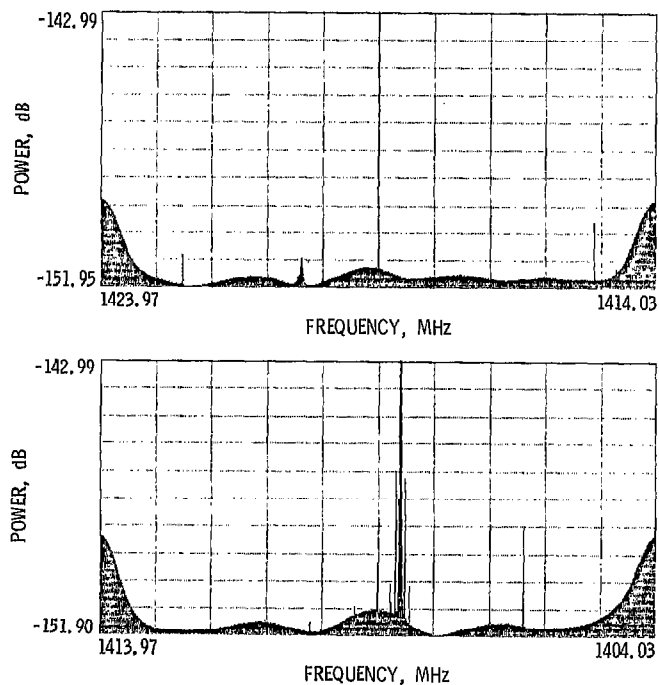


Fig. 2. Occurrences of RFI events versus azimuth in the 1404- to 1424-MHz frequency band





**Fig. 3. Relative power (logarithmic) vs frequency near longitude 111.1° on day 288 (1983); resolution = 16 kHz**



**Fig. 5. Relative power (logarithmic) vs frequency near longitude 131.5° on day 288 (1983); resolution = 16 kHz**

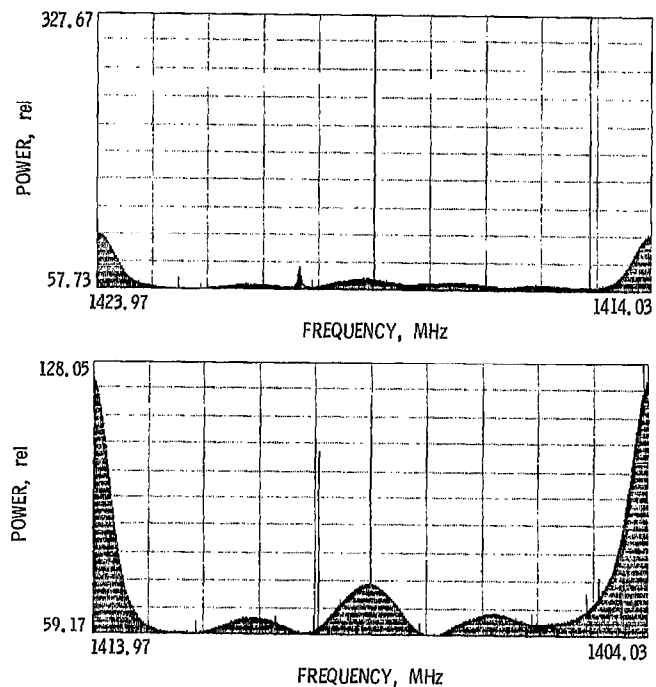


**Fig. 4. Relative power (linear) vs frequency near longitude 67.1° on day 283 (1983); resolution = 16 kHz**

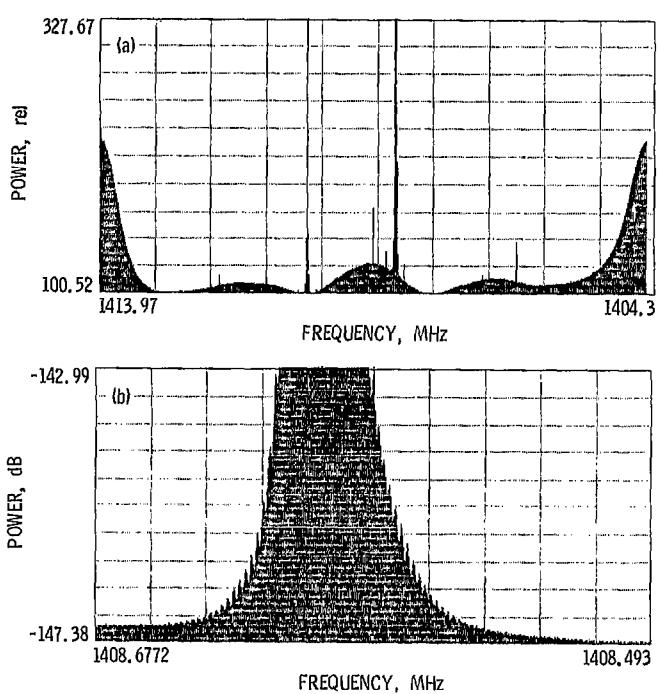


**Fig. 6. Relative power (linear) vs frequency near longitude 130.1° on day 271 (1983): (a) resolution = 16 kHz; (b) high resolution view of feature in (a) near 1408.6 MHz; resolution = 300 Hz**

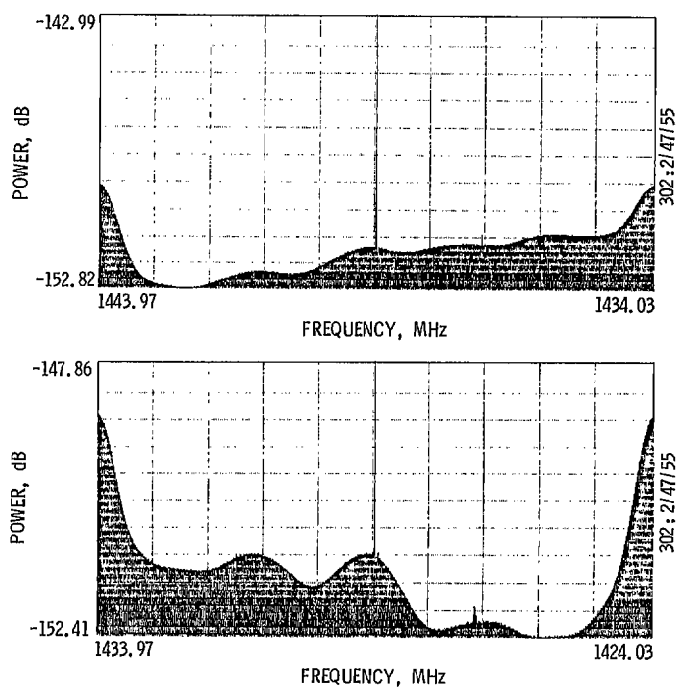


**Fig. 7. Relative power (logarithmic) vs frequency while tracking the Moon on day 302 (1983)**

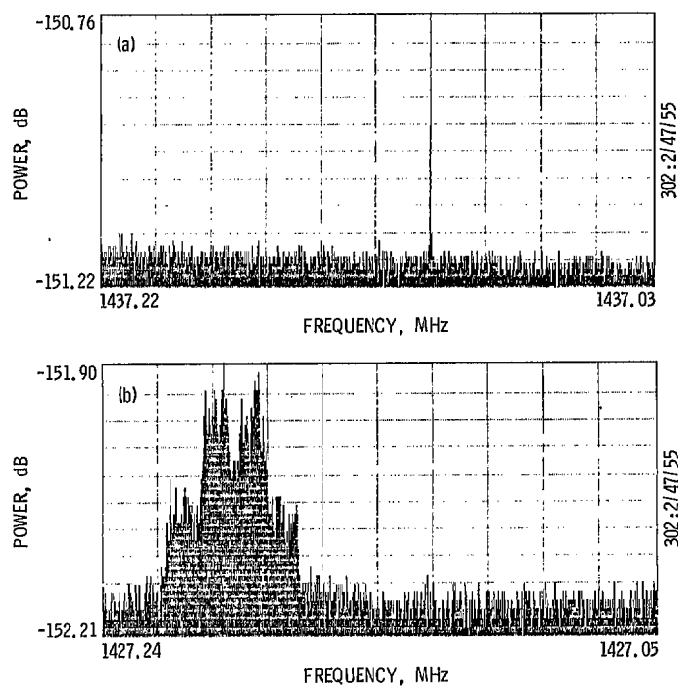


**Fig. 8. Relative power (logarithmic) vs frequency of two possible lunar echoes on day 302 (1983), resolution = 300 Hz: (a) signal near 1437 MHz; (b) signal near 1427 MHz**

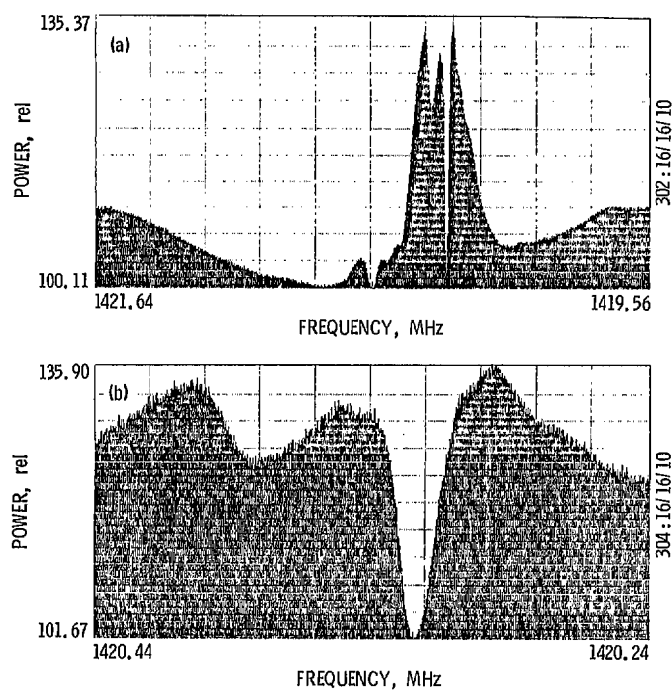


**Fig. 9. Relative power (linear) vs frequency of a complicated HI feature at the galactic center: (a) resolution = 3.4 kHz; (b) view of central HI feature; resolution = 320 Hz**